Nature Environment and Pollution Technology
An International Quarterly Scientific Journal

p-ISSN: 0972-6268
(Print copies up to 2016)
e-ISSN: 2395-3454

Vol. 22 | No. 1 | pp. 87-96 | 2023

Original Research Paper

https://doi.org/10.46488/NEPT.2023.v22i01.007

Open Access Journal

Corrosion Behavior of Petroleum Pipeline Steel in the Sulfur Ion Enriched Solution with Quinoline

Shanjian Li*(**)†, Guotao Cui*, Panfeng Wu*(**) and Yang Feng*****

*School of Chemistry and Chemical Engineering, Xi'an Shiyou University, Xi'an, 710065, PR of China

**Shaanxi Key Laboratory of Carbon Dioxide Sequestration and Enhanced Oil recovery, Xi'an 710065, Shaanxi, China

***No. 3 Gas production plant of Yanchang Gas Field of Shaanxi Yanchang Petroleum Co. Ltd., Yan'an, Shaanxi 716000, PR of China

†Corresponding author: Shanjian Li; lishanjian@xsyu.edu.cn

Nat. Env. & Poll. Tech.
Website: www.neptjournal.com

Received: 19-07-2022
Revised: 06-10-2022
Accepted: 18-10-2022

Key Words:
Local corrosion
Occluded battery
Quinoline corrosion inhibitor
Electrochemical behavior

ABSTRACT

Localized corrosion is a serious, hazardous destroyer of steel petroleum pipelines meant for long-time use. However, previous studies on localized corrosion primarily focused on local corrosion morphology and corrosion rate of bulk metals because detecting the corrosion state of occlusive metals is difficult. Herein, we employ a simulating occluded battery unit to disclose the local corrosion behavior of the steel petroleum pipeline (N80 steel) in an occlusive S^{2-}-enriched solution. After simulating localized corrosion in the S^{2-}- containing corrosion solution using the occluded battery unit, the occlusive solution was acidified and the migration amount of S^{2-} to the occluded area increased. Despite the increase of S^{2-} concentration, the addition of quinoline corrosion inhibitor (0.8 wt%) still effectively impedes the corrosion of the occluded metal. Moderately raising the environmental temperature can stimulate the activity of the inhibitor and promote the inhibition effect. The quinoline corrosion inhibitor displays the maximum inhibition rate at an elevated temperature of 50°C. Meanwhile, a maximum over the temperature of 60°C-70°C will likely accelerate the failure of the inhibitor.

INTRODUCTION

Amongst the various anti-corrosion methods for petroleum pipelines and equipment, the addition of corrosion inhibitors have been widely used due to their low cost, ease of operation, and convenience (Zong 2008, Wang 2017, Shi & Shi 2017, Jiao 2019, Xue & Liu 2018). Quinoline corrosion inhibitors are often used as acidizing corrosion inhibitors in petroleum exploitation to achieve a high corrosion inhibition rate, and satisfactory corrosion inhibition effect with low dosage (Puskullu et al. 2013, Ser et al. 2020, Chen et al. 2019, Dong et al. 2019). Previous reports confirmed that this type of corrosion inhibitor could effectively impede the uniform corrosion of metals (Huang et al. 2018, Lu et al. 2021, Yu & Zhen 2015). For instance, Wang et al. (2015) demonstrated the effect of 8-aminoquinoline and 8-nitroquinoline on the corrosion protection of AA5052 alloy in 3 wt% of NaCl solution using various experimental and computational methods. The 8-aminoquinoline and 8-NQ provided a protection efficiency of 89.5% and 87.0%, respectively. As anodic-type inhibitors, they can effectively enhance the value of charge transfer resistance to weaken the overall corrosion current on the metal at a concentration of 0.02 $mol.L^{-1}$. Upon a synergistic effect of 8-hydroxyquinoline with 0.4 wt% of KI, Obot et al. (2017) investigated the corrosion effect of 8-hydroxyquinoline on X60 steel in 15 wt% of HCl using loss-in-weight and electrochemical methods. The results showed satisfactory inhibition performance owing to the synergistically enhanced corrosion protection capability. Up till now, limited studies have been focused on the corrosion inhibition effect of quinoline corrosion inhibitors on the localized corrosion of metals.

Different from the above evaluation on uniform corrosion inhibition, herein, the corrosion inhibition of the quinoline corrosion inhibitor on the localized corrosion of N80 steel (a common material for oil pipelines) in Na_2S-containing oil and gas field mineralized water solution system is concentrated on by simulating the occluded battery method. S^{2-}- enriched and -acidized occlusive solutions are obtained, and their chemical state is analyzed in detail through the simulation method. The electrochemical corrosion behavior of N80 steel in the generated occluded solutions, along with changes in the chemical state of the occlusive solution, is explored. The corrosion state of this occlusive cell simulating the localized corrosion under elevated environmental temperature is

discussed to understand the quinoline-containing and S^{2-}-enriched systems further. This concentration on localized corrosion from the chemical state of the occlusive solution to the electrochemical corrosion state of the occlusive metal can provide a theoretical reference for the application of quinoline corrosion inhibitors to impede localized corrosion in the field of petroleum exploration and production.

MATERIALS AND METHODS

Materials

N80 steel used in this experiment is collected from Foshan Wenxian Electromechanical Control Company Limited. Analytical-grade sodium sulfide (Na_2S). The composition of mineralized water derived from oil and gas fields is listed in Table 1.

The corrosive medium is a mixed solution composed of 0, 1.0, 1.5, and 2.0 wt% Na_2S in oil and gas field mineralized water and prepared by dissolving the designed amount of Na_2S into the oil and gas field mineralized water.

Analytical Methods

Chemical evaluation of the occluded area: The simulated occluded battery was prepared according to our previous works (Li et al. 2016). The solution in the occlusive area was taken out for chemical analysis after the simulation of localized corrosion in the corrosive solution environment with/without quinoline quaternary ammonium salt. Initially, its pH value was measured after cooling to room temperature. The concentration of S^{2-} was then analyzed via titration. Before analysis, the same volume of sodium tetraphenylborate (7 $g.L^{-1}$) and potassium nitrate (7 $g.L^{-1}$) was added to the solution to remove the interference of quinoline quaternary ammonium salt.

The S^{2-} concentration was examined using iodometric titration according to the Chinese national standard of GB/T223.68-1997. The occlusive solution (0.25 mL) was pipetted to achieve a dilution of 100 mL using deionized water and then placed in a 250 mL Erlenmeyer flask. Sodium hydroxide (2 $g.L^{-1}$) and nitric acid (1+300000 $mg.L^{-1}$) solutions were mixed with the diluted solution to adjust the pH value and ensure that the red color just becomes colorless after adding two drops of phenolphthalein indicator (10 $g.L^{-1}$ of ethanol solution). Iodine standard solution (10 mL, 0.01 $mol.L^{-1}$) was then added to the mixture. Hydrochloric acid solution (5 mL, 18 wt%) was added dropwise to the mixture under continuous stirring to form a uniform blend. The blend was placed in a dark environment for 10 min. After titrating with sodium thiosulphate standard solution (0.01 $mol.L^{-1}$), it transformed into a light yellow solution from its original colorless appearance. The blend began to demonstrate a dark blue color after adding 1 mL of starch indicator solution (1.0 wt%). Titration was continued until the blue disappeared to indicate the endpoint. The S^{2-} concentration can be described in Equation 1.

$$\left[S^{2-}\right] = \frac{(V_0 - V_1) \times c}{V} \quad \ldots(1)$$

Where V_1 is the volume of sodium thiosulphate titrant consumed by the titration sample (mL), V_0 is the volume of sodium thiosulphate titrant consumed by the control sample (mL), V is the volume of the diluted occlusive solution (mL) and c is the molarity of the standard titration solution of sodium thiosulphate ($mol.L^{-1}$).

Table 1: Compositions of mineralized water.

Parameter	Measured value [$mg.L^{-1}$]
Ca^{2+}	1824.00
Mg^{2+}	169.59
Fe^{3+}	0.5492
Fe^{2+}	0.1727
Na^+ with K^+	1419.28
HCO_3^-	116.48
Cl^-	5843.22
SO_4^{2-}	7.56
pH	6.44

Electrochemical Evaluation

The polarization curve and alternating current (AC) impedance measurement on N80 steel in oil and gas field mineralized aqueous solutions with different concentrations of Na_2S and quinoline corrosion inhibitors were investigated using dynamic potential scanning and electrochemical impedance spectrum (EIS) methods. Based on these electrochemical evaluations, the uniform corrosion and localized corrosion behavior of N80 steel triggered by a specific corrosion medium and the inhibition effect of the corrosion inhibitor on the two corrosion forms are explored. Meanwhile, the corresponding corrosion inhibition mechanism of the corrosion inhibitor is analyzed. The corrosion inhibition rate derived from the polarization curve after testing is calculated as Equation 2, where η is the inhibition efficiency (%), I_{corr} is the corrosion current density without the corrosion inhibitor ($\mu A.cm^{-2}$) and I'_{corr} is the corrosion current density with the corrosion inhibitor ($\mu A.cm^{-2}$).

$$\eta = \frac{(I_{corr} - I'_{corr})}{I_{corr}} \times 100\% \quad \ldots(2)$$

The corrosion inhibition rate based on the EIS method is expressed as follows:

$$\eta = \frac{(R_p - R_p^0)}{R_p} \times 100\% \quad \ldots(3)$$

Where η is the inhibition efficiency (%), R_p and R_p^0 represent the polarization resistance with and without the corrosion inhibitor ($\Omega.cm^{-2}$), respectively.

RESULTS AND DISCUSSION

Simulating the Constant Current Experiment in the Occluded Battery

After simulating the occlusive corrosion of N80 steel at 50°C for 8 h, changes in the S^{2-} concentration and pH of the solution inside and outside the occlusion zone in different Na_2S oil and gas field-mineralized water systems are presented in Table 2.

Data in Table 2 indicate that the S^{2-} concentration in the occluded area is 1.05, 1.45, 1.38, and 1.16 times more concentrated than the original values in the oil and the gas field-mineralized water corrosion solution system with 0, 1.0, 1.5 and 2.0 wt% of Na_2S. Meanwhile, the pH value inside the occlusive solution drops sharply as the solution acidifies. A localized corrosion cell composed of an ultra-small anode (sample inside occluded area) interacting with a large cathode (sample outside occluded area) is formed when the anode current is applied to the simulated occlusion battery system. The anodic current accelerates the metal dissolution inside the occlusive area to generate high-concentration metal cations, which are hydrolyzed to produce a large amount of H^+. As a result, the pH value of the occlusive solution drops significantly. Due to the increased positive charge inside the occlusive area, S^{2-} in the outside bulk solution continuously migrates to the occlusive zone to maintain the electric neutrality of the solution. After adding different concentrations of the quinoline corrosion inhibitor to diverse oil and gas field-mineralized water systems with various concentrations of Na_2S, changes in the S^{2-} concentration and pH of the solution in the occluded area under the condition

Table 2: The composition changes of the solution inside/outside the occluded area in the oil and gas fields mineralized aqueous solution system with different concentrations of Na_2S.

Current density	Solution system	Sampling	S^{2-} concentration [mol.L^{-1}]	pH
i = 1 mA.cm^{-2}	0 wt% Na_2S + Oil and gas field mineralized water	Inside	0.2400	4.63
		Outside	0.2280	12.21
	1.0 wt% Na_2S + Oil and gas field mineralized water	Inside	0.3441	4.97
		Outside	0.2360	12.38
	1.5 wt% Na_2S + Oil and gas field mineralized water	Inside	0.3522	5.67
		Outside	0.2560	12.49
	2.0 wt% Na_2S + Oil and gas field mineralized water	Inside	0.3780	6.45
		Outside	0.3241	12.66

Table 3: Changes in solution composition of the occluded solution with different concentrations of corrosion inhibitor-modified Na_2S oil and gas field mineralization aqueous system.

Current density	Solution system	Inhibitor concentration [wt%]	S^{2-} concentration [mol.L^{-1}]	pH
i = 1 mA.cm^{-2}	0 wt% Na_2S + Oil and gas field mineralized water	0.0	0.2400	4.63
		0.2	0.0188	4.69
		0.5	0.0100	4.73
		0.8	0.0040	4.81
	1.0 wt% Na_2S + Oil and gas field mineralized water	0.0	0.3441	4.97
		0.2	0.0320	5.20
		0.5	0.0240	5.44
		0.8	0.0064	5.59
	1.5 wt% Na_2S + Oil and gas field mineralized water	0.0	0.3522	5.67
		0.2	0.0441	5.90
		0.5	0.0323	6.09
		0.8	0.0241	6.41
	2.0 wt% Na_2S + Oil and gas field mineralized water	0.0	0.3780	6.45
		0.2	0.1400	6.83
		0.5	0.1240	6.95
		0.8	0.1000	7.13

of simulating the occlusive corrosion at 50°C for 8 h are presented in Table 3.

The S^{2-} enrichment and solution acidification are alleviated by adding different concentrations of the quinoline corrosion inhibitor under the same corrosion current density. The trend curve of the S^{2-} concentration versus the corrosion inhibitor concentration is depicted in Fig. 1(a). Compared with that of the controlled solution without the inhibitor, the S^{2-} concentration decreases gradually with the increase of concentration of the corrosion inhibitor. This finding indicates that the corrosion of metals in the occlusive zone is mitigated and the dissolution of metal reduces. The S^{2-} concentration in the occlusive zone still decreases rapidly when 2.0 wt% of the quinoline corrosion inhibitor is added. The downward trend of the S^{2-} concentration slows down with the continued concentration increase of the corrosion inhibitor. The pH of the solution in the occlusive zone also clearly increases after adding a certain concentration of the corrosion inhibitor to the bulk solution, thereby showing an inverse trend to the S^{2-} concentration (Fig. 1(b)). The pH value of the occlusive solution in the four Na_2S oil and gas field mineralization aqueous systems gradually increases with the increase of the corrosion inhibitor concentration, thereby suggesting that the corrosion of the metal in the occlusive area is mitigated. Overall, this type of quinoline corrosion inhibitor can effectively reduce the migration of S^{2-} to the occlusive area whilst inhibiting solution acidification. Hence, the dissolution of metal in the occlusive area is prevented from slow down the occurrence of local corrosion.

Changes in the Electrochemical State of the Occluded Area

The simulated occluded battery unit in the four solution systems with different concentrations of corrosion inhibitors was operated at an anodic current density of 1 $mA.cm^{-2}$ for 8 h to generate the corresponding occlusive solutions before conducting the electrochemical measurement. The dynamic potential polarization curve was then obtained with the occluded sample of N80 petroleum special steel at 50°C in the formed occlusive environment (Fig. 2). The anodic polarization kinetic constant βa, cathodic polarization kinetic constant βc, self-corrosion current I_0, self-corrosion potential E_{corr}, corrosion rate fitted from Fig. 2(a)–2(d), and the calculated corrosion inhibition rate is listed in Table 3.

As illustrated in Fig. 2, the chemical state of the occluded area changes with the addition of the corrosion inhibitor. Upon adding corrosion inhibitors, the self-corrosion potential of N80 steel in the simulated occlusive solution shifts positively and both the self-corrosion current density and corrosion rate decrease significantly in the four solution systems. The metal corrosion rate in the occluded area decreases from 0.51 $mm.a^{-1}$ to 0.12 $mm.a^{-1}$ when 0.8 wt% of the quinoline corrosion inhibitor is added to the oil and gas field-mineralized aqueous solution system with 0 wt% of Na_2S. The corresponding corrosion inhibition rate is calculated at 77%. Similarly, the significantly reduced metal corrosion rate in the occluded area corresponds to a maximum corrosion inhibition rate of 83% and 86% in the oil and gas field mineralized aqueous solution systems with 1.0 and 1.5 wt% of Na_2S, respectively. The decrease of corrosion rate in the oil and gas field mineralization aqueous system containing 2.0 wt% of Na_2S slows down from 0.98 $mm.a^{-1}$ to 0.41 $mm.a^{-1}$, corresponding to a corrosion inhibition rate rebound of 58%. Although the concentration of S^{2-} in the solution system increases, the quinoline corrosion inhibitor can still inhibit the corrosion of the occluded area to a

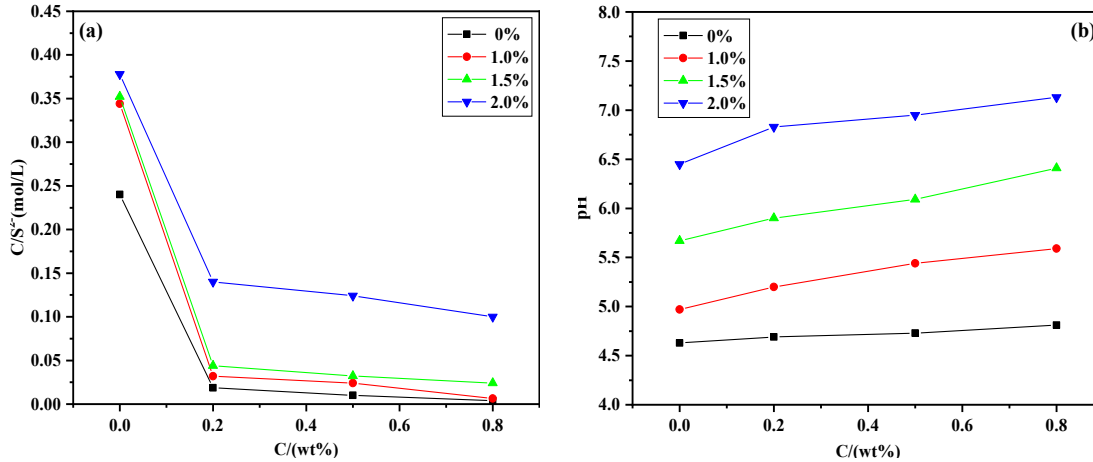

Fig. 1: (a) Trend curves of the change in S^{2-} concentration of the occlusive solution as the concentration of the corrosion inhibitor increases. (b) Variation of the pH of the occlusive solution with the concentration of the corrosion inhibitor.

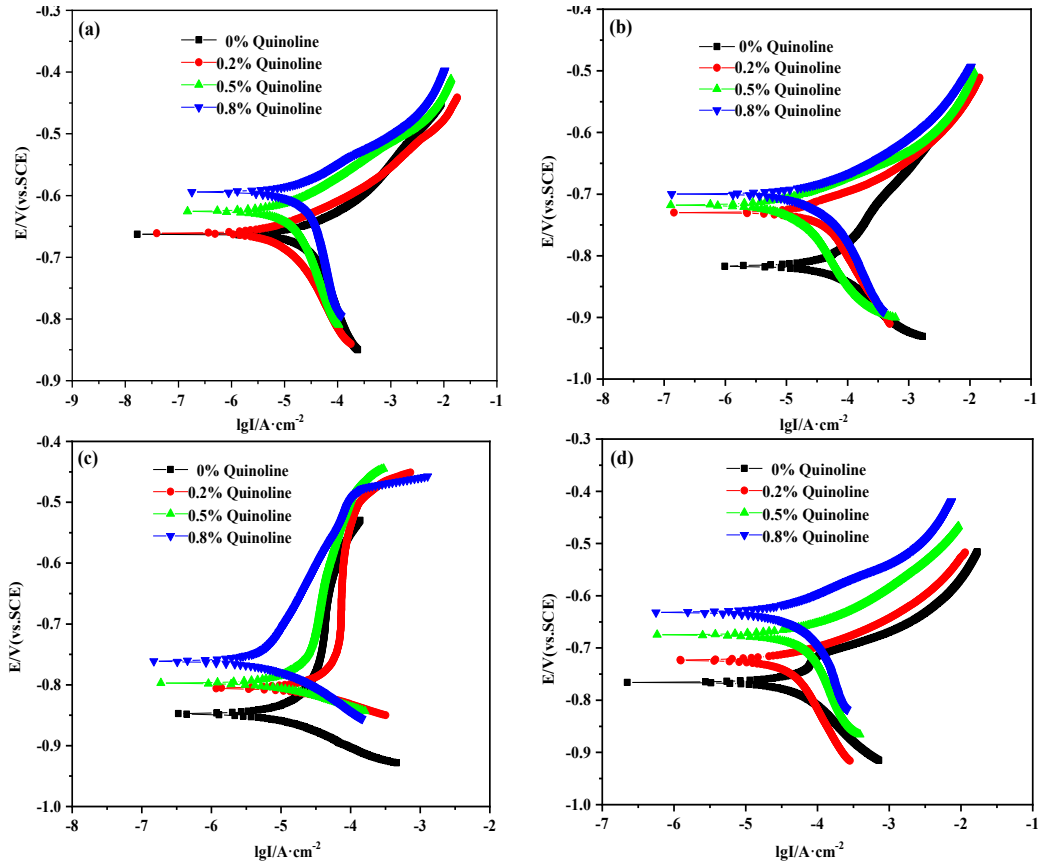

Fig. 2: Polarization curves tested in the occlusive area in oil and gas field-mineralized aqueous solution systems with (a) 0%, (b) 1.0%, (c) 1.5%, and (d) 2.0% of Na_2S after different concentrations of the corrosion inhibitor modification.

Table 3: Electrochemical parameters fitted from the polarization curves through potentiodynamic scanning.

Corrosion solution	Temperature [°C]	Inhibitor concentration [wt%]	Ba [mV]	Bc [mV]	E_0 [V]	I_0 [μA.cm^{-2}]	Corrosion rate [mm.a^{-1}]	Corrosion inhibition rate [%]
0 wt% Na_2S+Oil and gas field mineralized water	50	0.0	82.38	355.80	-0.6627	42.90	0.5046	---
		0.2	57.15	236.96	-0.6612	18.73	0.2204	56%
		0.5	60.04	213.82	-0.6254	14.00	0.1654	67%
		0.8	55.75	149.50	-0.5951	9.85	0.1158	77%
1.0 wt% Na_2S+Oil and gas field mineralized water	50	0.0	157.38	103.63	-0.8162	79.67	0.9371	---
		0.2	67.79	180.12	-0.7301	43.07	0.5066	46%
		0.5	58.73	129.43	-0.7180	18.71	0.2201	77%
		0.8	54.05	148.53	-0.7007	13.60	0.1599	83%
1.5 wt% Na_2S+Oil and gas field mineralized water	50	0.0	1709.90	63.74	-0.8479	63.50	0.7467	---
		0.2	453.82	75.570	-0.8056	22.78	0.2679	64%
		0.5	334.74	48.14	-0.7982	16.19	0.1905	74%
		0.8	309.65	72.89	-0.7620	8.67	0.1020	86%
2.0 wt% Na_2S+Oil and gas field mineralized water	50	0.0	86.54	386.70	-0.7657	83.41	0.9812	---
		0.2	74.80	485.82	-0.7239	69.16	0.8135	17%
		0.5	77.31	249.46	-0.6757	53.70	0.6316	36%
		0.8	71.16	114.07	-0.6315	35.03	0.4120	58%

certain extent. The corrosion inhibition rate of the quinoline corrosion inhibitor (0.8 wt%) to the occluded area still reaches 58% when the Na_2S content rises to a maximum of 2.0% in the solution system. These results indicate that the addition of the quinoline inhibitor to the bulk solution can highly benefit the electrochemical state of the occluded area by slowing down the corrosion of the metal in the occluded area to inhibit the occurrence and development of local corrosion.

The oil and gas field mineralized water system without Na_2S is taken as an example to discuss the influence of temperature on the corrosion behavior of N80 steel in the occlusion area. Fig. 3(a) and 3(b) illustrate the polarization curve of N80 steel tested in the occlusion zone solution at 40°C–70°C after simulating the localized corrosion for 8 h in the oil and gas field mineralization aqueous system with and without the addition of 0.8 wt% of the quinoline inhibitor. The fitted Tafel parameters, including βa, βc, $I_{0,}$ and E_{corr}, are listed in Table 4.

As shown in Fig. 3(a) and Table 4, the self-corrosion potential of the polarization curve measured in the occlusive solution without corrosion inhibitor negatively shifts from 40°C to 70°C, whilst the corrosion current density increases gradually. Both the negative shift of corrosion potential and the increase of corrosion current density slow down after adding 0.8 wt% of the quinoline corrosion inhibitor to the bulk solution. This finding indicates that the corrosion acceleration effect on both the cathode and anode is significantly alleviated by the inhibitor at elevated temperatures (Fig. 3(b)).

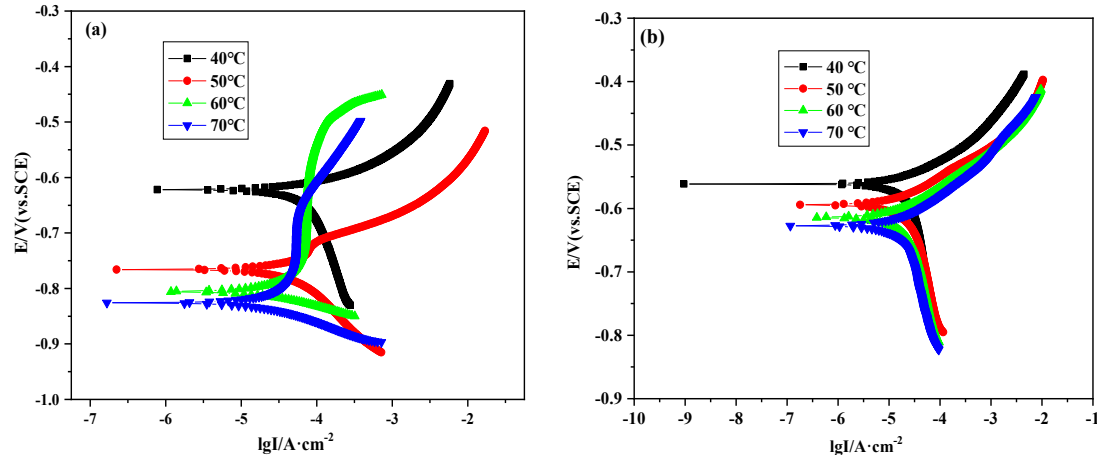

Fig. 3: Polarization curves tested in the occlusive solution of the oil and gas field mineralization aqueous solution system with 0 wt% of Na_2S (a) in the absence of corrosion inhibitor and (b) in addition of the corrosion inhibitor (0.8 wt%) at 40°C-70°C.

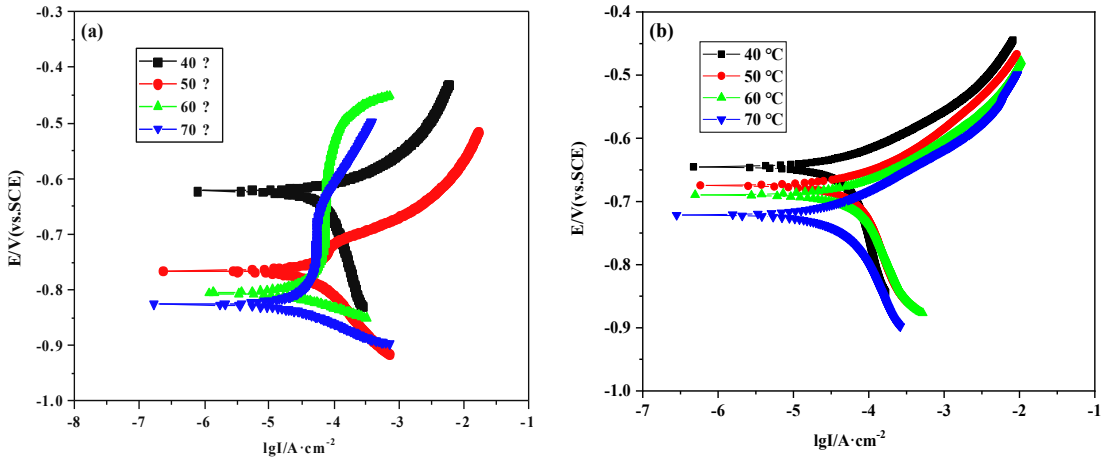

Fig. 4: Polarization curve tested in the occlusive solution in the oil and gas field mineralized aqueous solution system with 1.5 wt% of Na_2S (a) in the absence of the corrosion inhibitor and (b) in addition of 0.8 wt% of the corrosion inhibitor at 40°C-70°C.

Table 4: Parameters fitted from the polarization curve tested in two kinds of corrosion solution systems without/without corrosion inhibitor at 40-70°C.

Corrosion solution	Temperature [°C]	Inhibitor concentration [wt%]	E_0 [mV]	I_0 [μA.cm^{-2}]	Corrosion inhibition rate [%]
0 wt% Na_2S+Oil and gas field mineralized water	40	0.0	-645.58	55.50	
		0.8	-561.59	19.51	65%
	50	0.0	-662.69	42.90	
		0.8	-595.11	9.85	77%
	60	0.0	-688.71	41.49	
		0.8	-614.27	24.69	41%
	70	0.0	-716.08	35.59	
		0.8	-627.46	23.63	34%
1.5 wt% Na_2S+Oil and gas field mineralized water	40	0.0	-622.84	126.00	
		0.8	-645.50	64.33	49%
	50	0.0	-765.73	83.42	
		0.8	-631.49	35.03	58%
	60	0.0	-805.60	137.51	
		0.8	-690.55	77.27	44%
	70	0.0	-826.84	107.44	
		0.8	-721.29	67.23	37%

Increasing the Na_2S content to 1.5 wt% in the solution system, the inhibition effect of the quinoline corrosion inhibitor (0.8 wt%) is weakened slightly at elevated temperatures from 40°C to 70°C, as illustrated in Figs. 4(a) and 4(b). However, inhibition effectiveness, such as self-corrosion potential, corrosion current density, and corrosion inhibition rate, follows the same attenuation law as that in Figs. 3(a) and 3(b). Fitted parameters from the polarization curve of Fig. 4(a) and 4(b) shown in Table 4 0further reveal that the corrosion effect is inferior to that in the system without Na_2S and with 0.8 wt% of the quinoline corrosion inhibitor under the same environmental temperature. The corrosion inhibition rate reduces to 37% when the temperature is increased to 70°C. These electrochemical analyses demonstrated that the addition of the quinoline corrosion inhibitor to the bulk solution could efficiently mitigate the corrosion of the occluded metal, even at an elevated temperature of 50°C regardless of the Na_2S solution (0 or 1.5 wt%) used. Inhibition superiority is significantly impaired at a sufficiently higher temperature of 60°C–70°C. This finding indicates that an over temperature will likely accelerate the failure of the quinoline corrosion inhibitor.

Electrochemical Impedance Spectroscopy Analysis

Electrochemical impedance spectra measured in the occlusion zone solution after simulating the localized corrosion in the four corrosion solution systems at 50°C for 8 h are depicted in Fig. 5. Electrochemical impedance spectra (EIS) are fitted using the equivalent circuit model (Fig. 6), which is composed of a double-layer electric capacitance C_{dl} parallel to the polarization resistance R_p, which is in series with the former solution resistance R_s. EIS parameters are fitted using the equivalent circuit (Table 5).

Compared with the impedance spectrum of the controlled solution without corrosion inhibitor, the fitted diameter of the semicircle representing the polarization resistance R_p increases with the increase of the corrosion inhibitor concentration in the four solution systems, while the interface capacitance C_{dl} decreases (Fig. 5). This variation tendency indicated that the quinoline corrosion inhibitor diffuses smoothly from the bulk solution into the occlusive area and competitively adsorbs onto the surface of the steel to form a protective film while replacing water molecules and corrosive anions on the steel surface after adding quinoline into the bulk solution.

As shown in Table 5, the polarization resistance of the corrosion system increases while the interface capacitance C_{dl} decreases with the addition of the corrosion inhibitor at increasing concentrations to the bulk solution in the four solution systems due to the growing thickness of the adsorbed quinoline layer. Correspondingly, the calculated corrosion inhibition rate based on the polarization resistance increases gradually. The corrosion inhibitor still exerts an acceptable inhibitive effect on the occluded area with the increase of the S^{2-} concentration from the perspective of the corrosion medium. The addition of quinoline (0.8 wt%) to the oil and

Table 5: Fitted electrochemical impedance spectroscopy parameters.

Corrosion solution	Temperature [°C]	Inhibitor concentration [wt%]	R_s	C_{dl}	R_p	Corrosion inhibition rate [η]
0 wt% Na_2S+Oil and gas field mineralized water	50	0.0	18.91	1.33×10^{-3}	230.5	-
		0.2	7.51	5.77×10^{-5}	327.9	30%
		0.5	8.29	1.33×10^{-5}	712.5	68%
		0.8	4.65	3.31×10^{-4}	776.8	70%
1.0 wt% Na_2S+Oil and gas field mineralized water	50	0.0	7.21	2.50×10^{-3}	100.7	-
		0.2	4.51	6.70×10^{-3}	150.1	33%
		0.5	3.84	1.27×10^{-2}	158.6	37%
		0.8	8.97	2.74×10^{-3}	256.7	61%
1.5 wt% Na_2S+Oil and gas field mineralized water	50	0.0	10.49	9.14×10^{-4}	132.0	-
		0.2	4.88	4.2×10^{-3}	150.5	12%
		0.5	7.58	1.26×10^{-3}	211.8	38%
		0.8	17.34	9.14×10^{-4}	364.8	64%
2.0 wt% Na_2S+Oil and gas field mineralized water	50	0.0	7.62	2.48×10^{-3}	437.2	-
		0.2	4.67	5.61×10^{-4}	718.7	39%
		0.5	3.25	1.45×10^{-3}	1521.0	71%
		0.8	7.91	1.73×10^{-3}	2094.0	79%

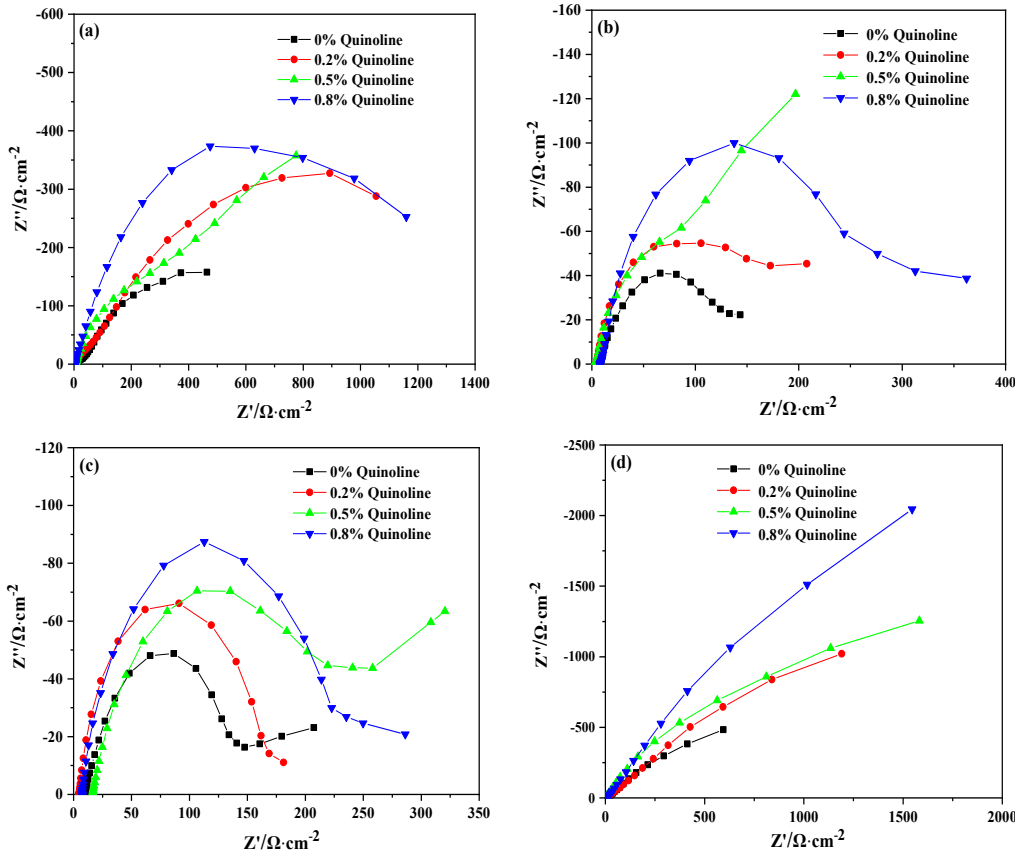

Fig. 5: EIS comparison in the blocked area of the oil and gas field mineralized aqueous solution systems with (a) 0 wt%, (b) 1.0 wt%, (c) 1.5 wt% and (d) 2.0 wt% of Na_2S at different concentrations of the corrosion inhibitor.

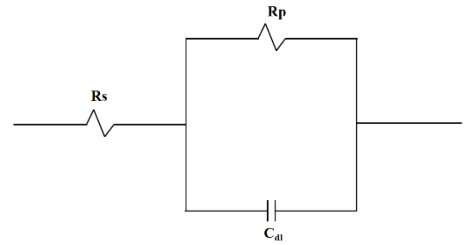

Fig. 6: Equivalent circuit diagram.
(Rs—solution resistance, Rp—polarization resistance, and Cdl—electric double-layer capacitance)

gas field mineralized water system with 2.0 wt% of Na_2S can significantly slow down the corrosion of the occluded metal. The corrosion rate with 0.8 wt% of quinoline can still reach 79% even at a high temperature of 50°C, indicating that quinoline can effectively inhibit the formation and expansion of local corrosion. This finding is consistent with the results of the polarization curve measurement.

CONCLUSIONS

In summary, the corrosion inhibition of the quinoline corrosion inhibitor on the localized corrosion of N80 steel in Na_2S-containing oil and gas field mineralized water solution system is investigated by simulating the occluded battery method. Through simulating the anodic polarization of the occluded battery in the corrosion solution, the solution in the occluded area is acidified as the pH drops sharply and an increasing amount of S^{2-} concentrates migrate into the occluded area simultaneously. Correspondingly, the S^{2-} concentrations in the occluded area of the oil and gas field mineralized water corrosion solution systems with 0, 1.0, 1.5, and 2.0 wt% of Na_2S are 1.05, 1.45, 1.38, and 1.16 times higher than the original values. The addition of the quinoline corrosion inhibitor can mitigate the acidification of the occlusive solution and the migration of S^{2-} to the occlusive zone. Hence, the dissolution of metal in the occlusive zone is alleviated against local corrosion. The electrochemical corrosion of N80 steel in the occluded area significantly slows down with the changes in the chemical state of the occlusive solution. The corrosion inhibitor can still effectively inhibit the corrosion of the occluded metal with an increase of the S^{2-} concentration in the system. Moderately raising the environmental temperature is beneficial for stimulating the activity of the inhibitor and promoting the inhibition effect. The quinoline corrosion inhibitor displays the maximum inhibition rate at an elevated temperature of 50°C, while an over the temperature of 60°C–70°C will likely accelerate the failure of the quinoline corrosion inhibitor.

ACKNOWLEDGEMENT

Author contributions: Shanjian Li was responsible for document preparation, data and statistical analyses, and figure generation. Guotao Cui, Panfeng Wu, and Yang Feng contributed to the study design, document framing, technical review, and editing.

Funding: This work was carried out with the financial support of the National Natural Science Foundation of China (21808182), Xi'an Science and Technology Plan Project Science and Technology Innovation Talent Service Enterprise Project (2020KJRC0096) and National Science Foundation of Shaanxi (2022GY-144). Open Foundation of Shaanxi Key Laboratory of Carbon Dioxide Sequestration and Enhanced Oil Recovery (No. YJSYZX22SKF0002)

Data availability statement: Data were presented in the main manuscript or the supplemental data and raw data were available on request from the corresponding author (lishanjian@xsyu.edu.cn).

REFERENCES

Chen, S., Chen, S. and Li, W. 2019. Corrosion inhibition effect of a new quinoline derivative on Q235 steel in H_2SO_4 solution. Int. J. Electrochem. Sci., 14: 11419-11428.

Dong, Q.C., Zhang, G.H. and Zhang, W.B. 2019. Experimental and theoretical analysis of quinoline Gemini quaternary ammonium salt corrosion inhibitor. Chem. J. Chin. Univ., 40(10): 2195-2204.

Huang, P., Liu, W.J. and Zhang, Q.D. 2018. Preparation and performance evaluation of new quinoline corrosion inhibitors. China Petrol. Chem. Stand. Qual., 38(14): 102-103.

Jiao, D.W. 2019. Problems in the corrosion protection of petroleum pipelines and their solutions. Total Corr. Contr., 33(05): 96-98.

Li, S.J., Feng, L.J. and Zhang, J. 2016. Corrosion study of quinoline derivative corrosion inhibitor on tubing steel in simulated solution occlusion area. J. Appl. Basic Eng. Sci., 24(05): 1025-1033.

Lu, Y., Feng, H.X. and Tang, R.P. 2021. Summary of research and application of quinoline and its derivatives in metal corrosion inhibitors. Plast. Addit., 3: 6-10.

Obot, I.B., Ankah, N.K., Sorour, A.A., Gasem, Z.M. and Haruna, K. 2017. 8-Hydroxyquinoline as an alternative green and sustainable acidizing oilfield corrosion inhibitor. Sust. Mater. Technol., 14: 1-10.

Puskullu, M.O., Tekiner, B. and Suzen, S. 2013. Recent studies of antioxidant quinolone derivatives. Mini Rev. Med. Chem., 13(3): 365-372.

Ser, C.T., Žuvela, P. and Wong, M.W. 2020. Prediction of corrosion inhibition efficiency of pyridines and quinolines on an iron surface using machine learning-powered quantitative structure-property relationships. Appl. Surf. Sci., 512: 145612.

Shi, Y.H. and Shi, Y.K. 2017. Analysis of influence factors of pipeline corrosion. Petrochem. Technol., 24(12): 115.

Wang, D., Yang, D., Zhang, D.Q., Li, K., Gao, L.X. and Lin, T. 2015. Electrochemical and DFT studies of quinoline derivatives on corrosion inhibition of AA5052 aluminium alloy in NaCl solution. Appl. Surf. Sci., 357: 2176-2183.

Wang, Z.Y. 2017. Analysis of corrosion factors of petroleum pipelines and optimization measures for corrosion protection. Chem. Manag., 21(08): 126-127.

Xue, S.X. and Liu, C. 2018. The current situation of the corrosion work of petroleum pipelines and the countermeasures. Chem. Eng. Design Newslett., 44(07): 27.

Yu, H.L. and Zhen, H. 2015. Study on the synthesis and performance of a quinoline-type corrosion inhibitor. Sci. Technol. Eng., 15(19): 106-109.

Zong, P. 2008. Study on the synthesis of quaternary ammonium salt type acidizing corrosion inhibitor and its corrosion inhibition mechanism. China Univ. Petrol., 11: 56.